NASA/TM—2005-213647

Validation of the NCC Code for Staged Transverse Injection and Computations for a RBCC Combustor

Kumud Ajmani
Taitech, Inc., Beavercreek, Ohio

Nan-Suey Liu
Glenn Research Center, Cleveland, Ohio

July 2005

The NASA STI Program Office . . . in Profile

Since its founding, NASA has been dedicated to the advancement of aeronautics and space science. The NASA Scientific and Technical Information (STI) Program Office plays a key part in helping NASA maintain this important role.

The NASA STI Program Office is operated by Langley Research Center, the Lead Center for NASA's scientific and technical information. The NASA STI Program Office provides access to the NASA STI Database, the largest collection of aeronautical and space science STI in the world. The Program Office is also NASA's institutional mechanism for disseminating the results of its research and development activities. These results are published by NASA in the NASA STI Report Series, which includes the following report types:

- TECHNICAL PUBLICATION. Reports of completed research or a major significant phase of research that present the results of NASA programs and include extensive data or theoretical analysis. Includes compilations of significant scientific and technical data and information deemed to be of continuing reference value. NASA's counterpart of peer-reviewed formal professional papers but has less stringent limitations on manuscript length and extent of graphic presentations.

- TECHNICAL MEMORANDUM. Scientific and technical findings that are preliminary or of specialized interest, e.g., quick release reports, working papers, and bibliographies that contain minimal annotation. Does not contain extensive analysis.

- CONTRACTOR REPORT. Scientific and technical findings by NASA-sponsored contractors and grantees.

- CONFERENCE PUBLICATION. Collected papers from scientific and technical conferences, symposia, seminars, or other meetings sponsored or cosponsored by NASA.

- SPECIAL PUBLICATION. Scientific, technical, or historical information from NASA programs, projects, and missions, often concerned with subjects having substantial public interest.

- TECHNICAL TRANSLATION. English-language translations of foreign scientific and technical material pertinent to NASA's mission.

Specialized services that complement the STI Program Office's diverse offerings include creating custom thesauri, building customized databases, organizing and publishing research results . . . even providing videos.

For more information about the NASA STI Program Office, see the following:

- Access the NASA STI Program Home Page at ***http://www.sti.nasa.gov***

- E-mail your question via the Internet to help@sti.nasa.gov

- Fax your question to the NASA Access Help Desk at 301–621–0134

- Telephone the NASA Access Help Desk at 301–621–0390

- Write to:
  NASA Access Help Desk
  NASA Center for AeroSpace Information
  7121 Standard Drive
  Hanover, MD 21076

NASA/TM—2005-213647

Validation of the NCC Code for Staged Transverse Injection and Computations for a RBCC Combustor

Kumud Ajmani
Taitech, Inc., Beavercreek, Ohio

Nan-Suey Liu
Glenn Research Center, Cleveland, Ohio

National Aeronautics and
Space Administration

Glenn Research Center

July 2005

Acknowledgments

The authors would like to acknowledge the use of the data obtained from Mark Stewart and Ambady Suresh, NASA Glenn Research Center, for the RBCC-combustor, and for many useful discussions.

Available from

NASA Center for Aerospace Information
7121 Standard Drive
Hanover, MD 21076

National Technical Information Service
5285 Port Royal Road
Springfield, VA 22100

Available electronically at http://gltrs.grc.nasa.gov

Validation of the NCC Code for Staged Transverse Injection and Computations for a RBCC Combustor

Kumud Ajmani
Taitech Inc.
Beavercreek, Ohio 45430

Nan-Suey Liu
National Aeronautics and Space Administration
Glenn Research Center
Cleveland, Ohio 44135

Abstract

The NCC code was validated for a case involving staged transverse injection into Mach 2 flow behind a rearward facing step. Comparisons with experimental data and with solutions from the FPVortex code were performed to assess the performance of the NCC code. The code was then used to perform computations to study fuel-air mixing for the combustor of a candidate rocket-based combined cycle engine geometry. Comparisons with a one-dimensional analysis and a three-dimensional code (VULCAN) were performed to assess the qualitative and quantitative performance of the NCC solver.

1. Introduction

NASA has been focusing on several alternative propulsion concepts in order to reduce the cost of access to space. Under NASA's Integrated Space Plan three key technologies are being studied: scramjet, Rocket-Based Combined Cycle (RBCC) and Turbine-Based Combined Cycle (TBCC).

The Integrated Systems Test of an Airbreathing Rocket (ISTAR) project is proposing to use the RBCC concept of combining rocket-based propulsion with dual-mode RAM/SCRAM air-breathing propulsion to create a strut-jet engine. This engine would combine rocket-containing struts with conventional combustor ducts to obtain high combustion efficiencies

in all flight regimes. RBCC engines take advantage of the synergistic interactions between the rocket and airbreathing elements of the engine and the use of high specific-impulse cycles to yield a mission-averaged specific impulse that is higher than all-rocket technology.

High-fidelity predictions of the physics for RBCC-combustor phenomena could be attained by the solution of Navier-Stokes equations for reacting flows, and this is a very challenging computational task. The complexity of fuel-air mixing in conjunction with large heat-release due to combustion is magnified by the combination of high-speed rocket exhaust flows and the relatively low-speed duct flows.

Recent work by Steffen et. al[1] has focused on the analysis of a typical RBCC system during rocket-only operation. The authors had performed an extensive numerical study to determine the parameters that would affect rocket-mode RBCC performance. The authors had determined that the expansion and combustion process downstream of the rocket nozzle could greatly impact the overall cycle specific-impulse. Stewart and Suresh[2] have performed multidisciplinary analysis of an ISTAR/RBCC configuration using the VULCAN code[3]. Their results will serve as a basis of comparison for the results in the current report. Daines and Segal[4] have identified rocket-enhanced mode performance, flame-holding and thermal choking as important issues for RBCC engines. These issues can only be effectively studied by detailed, high-fidelity analyses of RBCC combustor dynamics.

One of the challenges facing the designers in the ISTAR project is the lack of tools to quickly assess the combustion efficiency of proposed designs. In a typical design cycle, the design team may typically require answers to questions like - what impact will a particular fuel/air ratio have on combustion efficiency and how will the location and size of the injectors affect mixing in the combustor?

These and many other questions require robust and accurate computational tools which can provide reliable answers for the designers in order to help them reduce the size of the design space and also eliminate 'show-stopping' design paths early in the design cycle. The purpose of this report is to document the performance of a combustion simulation tool, the National Combustion Code (NCC), in providing answers to combustion design

issues for RBCC-type applications.

The report is organized into four sections. The introduction section is followed by a very brief description of the NCC code — the governing equations, spatial discretizations, and turbulence and chemistry modeling. This section is followed by validation studies for staged transverse injection into a supersonic throughflow behind a rearward-facing step. A comparison of computational and experimental results are then presented for the validation case. The computational results for a candidate RBCC-combustor are then presented. The results are compared with the computational results of two other codes. The final section is a summary of the present work.

2. Computational Tools

The National Combustion Code (NCC)[5] is a state-of-the-art computational tool which is capable of solving the time-dependent, Navier-Stokes equations with chemical reactions. The NCC is being developed primarily at NASA Glenn in order to support combustion simulations for a wide range of applications, and has been extensively validated and tested for low-speed chemically reacting flows.

2.1 Governing Equations

The Navier-Stokes equations for unsteady, compressible, chemically reacting gas flow with N species can be written as

$$\Gamma\frac{\partial\hat{Q}}{\partial\tau}+\frac{\partial Q}{\partial t}+\frac{\partial(F-F_v)}{\partial x}+\frac{\partial(G-G_v)}{\partial y}+\frac{\partial(H-H_v)}{\partial z}=I \tag{1}$$

where the vectors $Q, F, G, H, F_v, G_v, H_v$ and I are defined as

$$Q=(\rho,\rho u,\rho v,\rho w,\rho E,\rho\kappa,\rho\epsilon,\rho Y_1,\cdots,\rho Y_{N-1})^T$$

$$F=(\rho u,\rho u^2+p_g,\rho uv,\rho uw,(\rho E+p)u,\rho u\kappa,\rho u\epsilon,\rho uY_1,\cdots,\rho uY_{N-1})^T$$

$$G = (\rho v, \rho uv, \rho v^2 + p_g, \rho vw, (\rho E + p)v,$$
$$\rho v\kappa, \rho v\epsilon, \rho vY_1, \cdots, \rho vY_{N-1})^T$$

$$H = (\rho w, \rho uw, \rho vw, \rho w^2 + p_g, (\rho E + p)w,$$
$$\rho w\kappa, \rho w\epsilon, \rho wY_1, \cdots, \rho wY_{N-1})^T$$

$$F_v = (0, \tau_{xx}, \tau_{xy}, \tau_{xz}, u\tau_{xx} + v\tau_{xy} + w\tau_{xz} + q_{x_e},$$
$$\tau_{x\kappa}, \tau_{x\epsilon}, q_{x_1}, \cdots, q_{x_{N-1}})^T$$

$$G_v = (0, \tau_{xy}, \tau_{yy}, \tau_{yz}, u\tau_{xy} + v\tau_{yy} + w\tau_{yz} + q_{y_e},$$
$$\tau_{y\kappa}, \tau_{y\epsilon}, q_{y_1}, \cdots, q_{y_{N-1}})^T$$

$$H_v = (0, \tau_{xz}, \tau_{yz}, \tau_{zz}, u\tau_{xz} + v\tau_{yz} + w\tau_{zz} + q_{z_e},$$
$$\tau_{z\kappa}, \tau_{z\epsilon}, q_{z_1}, \cdots, q_{z_{N-1}})^T$$

$$I = (0, S_u, S_v, S_w, S_h, S_\kappa, S_\epsilon, S_1, \cdot, S_i, \cdot, S_{N-1})^T$$

where $\rho, p_g, u, v, w, E, \kappa, \epsilon$ and Y_i represent the density, gauge pressure, x-, y-, z- cartesian velocity components, total energy $(e + \frac{1}{2}(u^2 + v^2 + w^2))$, turbulent kinetic energy (TKE), dissipation rate of TKE, and species mass-fraction, respectively. The source terms $S_u, S_v, S_w, S_h, S_\kappa, S_\epsilon$ arise from a non-linear $\kappa - \epsilon$ turbulence model, and the source terms S_i are the chemical source terms for species i.

In order to overcome potential convergence problems for low Mach number flows, a preconditioning term $(\Gamma \frac{\partial \hat{Q}}{\partial \tau})$ has been added to the standard Navier-Stokes equations[6]. During the solution procedure, this term is driven to zero as the solver marches in pseudo-time, τ. In addition, the pressure term has been decomposed as a reference pressure (p_0) and a gauge (or fluctuating) pressure (p_g), i.e. $p = p_0 + p_g$. The vector $\hat{Q}$ is thus the vector of *primitive* dependent variables

$$\hat{Q} = (p_g, u, v, w, h, \kappa, \epsilon, Y_1, \cdots, Y_{N-1})^T$$

and the preconditioning matrix Γ is written as

$$\begin{bmatrix}
1/\beta & 0 & 0 & 0 & 0 & 0 & 0 & . & . & . & . & 0 \\
u/\beta & \rho & 0 & 0 & 0 & 0 & 0 & . & . & . & . & 0 \\
v/\beta & 0 & \rho & 0 & 0 & 0 & 0 & . & . & . & . & 0 \\
w/\beta & 0 & 0 & \rho & 0 & 0 & 0 & . & . & . & . & 0 \\
H/\beta - 1 & \rho u & \rho v & \rho w & \rho & 0 & 0 & . & . & . & . & 0 \\
\kappa/\beta & 0 & 0 & 0 & . & \rho & . & . & . & 0 & . & 0 \\
\epsilon/\beta & 0 & 0 & 0 & . & . & \rho & . & . & . & 0 & 0 \\
Y_1/\beta & 0 & 0 & 0 & 0 & . & . & \rho & . & . & . & 0 \\
Y_2/\beta & 0 & 0 & 0 & 0 & 0 & . & . & \rho & . & . & 0 \\
. & . & . & . & . & . & 0 & . & . & \rho & . & 0 \\
. & . & . & . & . & . & . & 0 & . & . & \rho & 0 \\
Y_{N-1}/\beta & 0 & 0 & 0 & . & . & . & . & 0 & . & . & \rho
\end{bmatrix}$$

where β is a scaling factor for the eigenvalues, and is computed as $\beta = u^2 + v^2 + w^2$. This ensures that all eigenvalues are of the same order of magnitude[7].

2.2 Time-Integration

Equation (1) is integrated volumetrically by applying a cell-centered, finite-volume discretization.

$$\begin{aligned}
&\Gamma \frac{\partial \hat{Q}}{\partial \tau} \Delta v + \frac{\partial Q}{\partial t} \Delta v + \\
&\sum_{n=1}^{nf} (F - F_v) A_x + \sum_{n=1}^{nf} (G - G_v) A_y + \\
&\sum_{n=1}^{nf} (H - H_v) A_z = I \Delta v
\end{aligned} \tag{2}$$

where Δv is the volume of the computational element, and nf is the number of faces constituting the element. A_x, A_y, A_z are the projections of the face area in the x, y, and z directions, respectively. Second-order accurate central-differences are used for the inviscid and viscous flux discretizations,

and a Jameson operator[8] (a blend of 2nd and 4th-order dissipation terms) is used to maintain numerical stability. In order to enhance convergence acceleration in pseudo-time, implicit residual smoothing is used to smooth the computed residuals. Turbulence-closure is obtained by a low-Reynolds number two-equation $k - \epsilon$ model[9]. For a steady state solution, $\frac{\partial Q}{\partial t}$ is set to zero, and equation (1) is integrated in pseudo-time with an explicit four-stage Runge-Kutta algorithm.

3. Test Results and Discussion

The National Combustion Code (NCC) is used to perform simulations of cross-flow injection in high-speed flows. A validation case was used to establish the performance of the NCC and the results compared with experimental and computational data. A candidate RBCC-combustor geometry was then computed with the NCC and the results compared with two other computational codes.

3.1 Validations Study: Staged Transverse Injection

The staged normal injection of two jets located behind a rearward-facing step into a Mach 2 freestream airflow is computed as the validation case. Experimental data for this configuration was obtained by McDaniel[10]. The computational setup for this problem is shown in figure 1. The mesh, with about 150,000 tetrahedal elements, is identical to the mesh used to compute this problem with the FPVortex code[11]. This would allow a one-to-one comparison between the current NCC computation and the FPVortex computation.

The geometry consists of a channel with a 3.18mm(=H) step and two 1.93mm(=D) injectors positioned on the channel centerline at 3 and 7 step-heights, respectively, downstream of the step. The channel height is 11.03 injector diameters (D) and the width is 15.79 injector diameters. The freestream flow conditions correspond to a stagnation temperature of 300K and stagnation pressure of 274KPa. The inflow boundaries for the main flow and the two injectors were set as fixed, specified inflow conditions. All flow variables were extrapolated at the outflow boundary.

The NCC computed contours on the z=0 plane (centerline of jets) for axial velocity and static pressure are shown in figure 2. The penetration of the two jets into the main flow is indicated in figure 3 (marker concentration contours of the two jets). Mach number contours and the concentration of the main flow marker are shown in figure 4.

Comparisons of the experimental data with the NCC and FPVortex computed normalized streamwise velocity and normalized static pressure profiles at various axial locations are shown in figures 5– 14. The locations of the upstream and downstream jets correspond to X/D=0.0 and X/D=6.6, respectively. The normalized velocity and pressure predicted by the NCC is qualitatively similar to the predictions of the FPVortex code, with some differences in the near wall regions. Note that the computational grid and flow and boundary conditions are identical for the NCC and FPVortex codes. The only probable difference between the two computations is the turbulence model. Overall, it may be concluded that the current NCC computations compare fairly well with available experimental and computational data.

3.2 RBCC Combustor Computations

Scram combustion within an RBCC-combustor configuration is modeled as a test case to evaluate the computational performance of the NCC code for high-speed combustor flows. The 'E-201' combustor configuration of the ISTAR vehicle is modeled, and the results are qualitatively compared with the computations performed with the VULCAN code[3] by Stewart and Suresh[2]. Comparisons are also made for certain flow quantities with a 1-D analysis with the FAST code[12]. The current NCC computation focuses on studying the mixing of the fuel (normal injection) with the secondary-air/rocket-exhaust main-stream flow.

The schematic for the current NCC computations is shown in figure 15. The current computation corresponds to a flight Mach Number of 3.5 (50K ft) with p_{tot}=77.4psi and T_{tot}=1345.5R. These conditions were used to specify the inflow conditions for the secondary flow (air). Subsonic flow conditions with p_{tot} and T_{tot} held fixed and Mach number allowed to float

(with an initial value of M=0.63) were used. The flow conditions for the (six) rocket faces correspond to rocket exhaust conditions of u=7930ft/s, T=2390R, ρ=0.0239lbm/ft^3. The rocket faces were specified with fixed, supersonic inflow conditions. The specified mass fractions of the species are $C_2H_4 = 0.05162$, $O_2 = 0.15885$, $CO_2 = 0.2289$, $H_2O = 0.56059$. The chemical reactions were modeled with a 6-species, 3-step, finite-rate reduced mechanism for ethylene described below. No turbulence-chemistry interactions were modeled in the current simulation.

Reactants	A_f	α_f	E_f
$C_2H_4 + O_2 \rightleftharpoons 2CO + 2H_2$	2.10E14	0.00	1.80153E4
$2CO + O_2 \rightleftharpoons 2CO_2$	3.48E11	2.00	1.013486E4
$2H_2 + O_2 \rightleftharpoons 2H_2O$	3.00E20	-1.00	0.0

The fuel is injected normal to the main flow (mixture of secondary air and rocket exhaust) at a downstream location through two transverse injectors of 0.331in effective diameter. The injection is sonic, with $p_{tot} = 531.2psi$, $T_{tot} = 1260R$ and $U_{inj} = 1615.22ft/s$. The injectors are gridded as triangular slots with matching area, momentum, and mass flow.

Computational results for the NCC code were compared with two previous computations with a 1-D code (FAST) and a 3-D code (VULCAN) as reported by Stewart and Suresh[2]. The VULCAN simulation used 1.02 million nodes, and was spatially first-order accurate. The current NCC computation uses 85,154 elements and is spatially second-order accurate. The chemistry model and flow conditions used for the current computation are identical to those used in the VULCAN simulation. A tabular comparison of area-averaged secondary-inflow quantities for the three computations is shown in Table 1. All the quantities are non-dimensionalized with the respective values reported from computations with the FAST code.

Quantity	FAST	VULCAN	NCC(current)
mdot	1.00	1.170	1.096
ptot	1.00	1.0373(fixed)	1.0373(fixed)
Ttot	1.00	1.0193(fixed)	1.0193(fixed)
Mach Number	1.00	1.2365	1.0635
Static Pres	1.00	0.9073	0.9642
Static Temp	1.00	0.9789	0.9837

Table 1. Area-averaged secondary-inflow quantities

A tabular comparison of area-averaged flow quantities at the internal nozzle exit plane is shown in Table 2.

Quantity	FAST	VULCAN	NCC(current)
mdot	1.00	1.1239	1.0264
Mach Number	1.00	0.9546	0.9897
Static Pres	1.00	1.2426	1.6800
Static Temp	1.00	0.9896	1.0094

Table 2. Area-averaged flow quantities at nozzle exit plane

A plot of the static temperature contours in a plane containing the centerline of the injector face(s) as computed by Stewart and Suresh with the VULCAN code is shown in figure 16. The plot shows that there is considerable penetration of the fuel jets into the main chamber, and fairly uniform burning downstream of the injectors. Note that the fuel penetration reported in many experiments (such as the one shown in figure 3) is typically more limited than the penetration shown in figure 16.

Figure 17 shows the fuel mass-fraction and temperature contours for the current NCC computation at y/Y=0.5 (injector center-line plane). Note that 'Y' is the distance between the symmetry face and the side-wall (see fig. 15). Also, y/Y=0 at the symmetry face and y/Y=1 at the side-wall. The current results differ from the Vulcan solution in two ways - the limited penetration of the fuel jets into the main flow, and the non-uniform burning downstream of the injectors. The current results show a distinct, low-temperature core-flow surrounded by two streams of hot flow in the vicinity of the upper and lower walls. The maximum temperature is 2247K, as

compared to 2870K reported in the VULCAN simulation.

One major difference between the VULCAN and NCC simulation is the mesh size and the mesh distribution. The VULCAN simulation used a structured, multiple-block approach with 1.02 million mesh points while the current NCC computation uses a unstructured mesh approach with only 85154 mesh points. This could possibly account for the differences in the two solutions. In order to somewhat further study this possibility, a second NCC computation was performed with a 225,204 element tetrahedral mesh. This finer mesh was obtained by doubling the number of points which represent the edges of the computational domain. The finer mesh does provide somewhat improved near-wall resolution. The fuel mass-fraction and temperature contours for the finer grid computations are shown in figure 18. There is no significant difference between the coarse and fine grid solutions. The jet penetration and fuel-air mixing characteristics are qualitatively the same for the fine and coarse grid computations. Hence, the grid size and/or distribution is ruled out as the major source of the difference between the current NCC computations and the previously reported VULCAN results.

Figures 19 and 20 show contours for fuel and H_2O mass-fractions at four different spanwise locations of the RBCC combustor. These locations were chosen to study the spanwise variation (y-axis of figure 15) in the combustor flow-field. Recall that y/Y=0 at the symmetry face and y/Y=1 at the side wall (fig. 15). The figures show that there is considerable variation in fuel-penetration and product formation at the different spanwise locations. The lack of mixing between the flow near the walls and the center of the combustor is very apparent at all four locations. This would suggest that a better mixing strategy would probably be required to enhance mixing and combustion efficiency. Figures 21 and 22 show contours for CO and CO_2 mass-fractions. The production of CO and CO_2 also varies considerably across the combustor. Figures 23 and 24 show contours for mach-number and pressure. The mach-number and pressure both change considerably as the flow moves downstream from the fuel injectors. The computed results are further illustrated in figures 25–32, which show the distribution of static temperature, static pressure, axial velocity, Mach number, and various species fractions at different axial locations.

4. Conclusions and Future Work

A successful computational study was conducted to validate and then apply the National Combustion Code (NCC) to high speed combustor problems with transverse fuel injection. The RBCC-combustor computations showed that the NCC code could prove to be a viable tool for high-fidelity analysis of combustor geometries. The comparison of NCC computations with experimental data and three other computation codes demonstrated that the NCC code compared fairly well for the class of problems studied. While there were some significant differences in the detailed flowfield between the NCC and Vulcan results for the RBCC-combustor geometry, the comparison of area-averaged quantities was fairly close. It would be interesting to revisit the comparisons when experimental data for this particular geometry becomes available.

5. Acknowledgements

The authors would like to acknowledge the use of the data obtained from Mark Stewart and Ambady Suresh at NASA GRC for the RBCC-combustor, and for many useful discussions.

6. References

1. Steffen, C.J. Jr., Smith, T.D., Yungster, S., and Keller, D.J., "Computational Analysis for Rocket-Based Combined-Cycle Systems During Rocket-Only Operation," *J. Propulsion and Power*, Vol. 16, No. 6, pp. 1030–1039 (2004).

2. Stewart, M.E.M., Suresh, A., Liou, M.-S., and Owen, A.K., "Multidisciplinary Analysis of a hypersonic engine," AIAA Paper 2002-5127 (2002).

3. White, J.A., "VULCAN User Manual," Version 4.3, March 2002, NASA Langley Research Center, Hampton, Virginia.

4. Daines, R., and Segal, C., "Combined Rocket and Airbreathing Propulsion Systems for Space-Launch Application," *J. Propulsion and Power*, Vol. 14, No. 5, pp. 605–612 (2004).

5. Moder, J. P. and NCC Team, "National Combustion Code: User Guide," March 2001, NASA Glenn Research Center.

6. Turkel, E., "Preconditioned Methods for Solving the Incompressible and Low Speed Compressible Equations," *AIAA Journal*, Vol. 21, pp. 1467-1475 (1983).

7. Chen, K.-H., and Pletcher, R. H., "Primitive Variable, Strongly Implicit Calculation Procedure for Viscous Flows at All Speeds," *AIAA Journal*, Vol. 29, No. 8, pp. 1241-1249 (1991).

8. Jameson, A., "Time Dependent Calculations using Multigrid, with applications to Unsteady Flows past Airfoils and Wings," AIAA Paper 91-1596 (1991).

9. Shih, T.-H., Chen, K.-H., and Liu N.-S., "A non-linear k-epsilon model for Turbulent Shear Flows," AIAA Paper 98-3983 (1998).

10. McDaniel, J.M., Fletcher, D., Hartfield, R., Jr., and Hollo, S., "Staged Transverse Injection into Mach 2 Flow Behind a Rearward Facing Step," AIAA Paper 91-5071 (1991).

11. Ebrahimi, H.B., Ryder, R.C., Jr., Brankovic, A., and Liu, N.-S., "A Measurement Archive for Validation of the National Combustion Code," AIAA Paper 2001-0811 (2001).

12. Faulkner, Robert F., "Integrated Systems Test of an Airbreathing Rocket (ISTAR)," AIAA Paper 2001-1812 (2001).

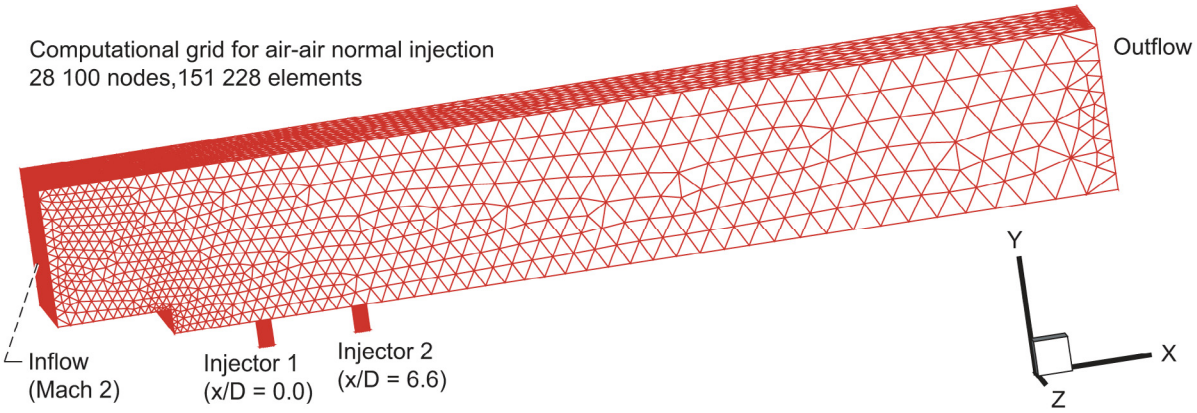

Figure 1.—Computational setup for transverse staged (sonic) injection.

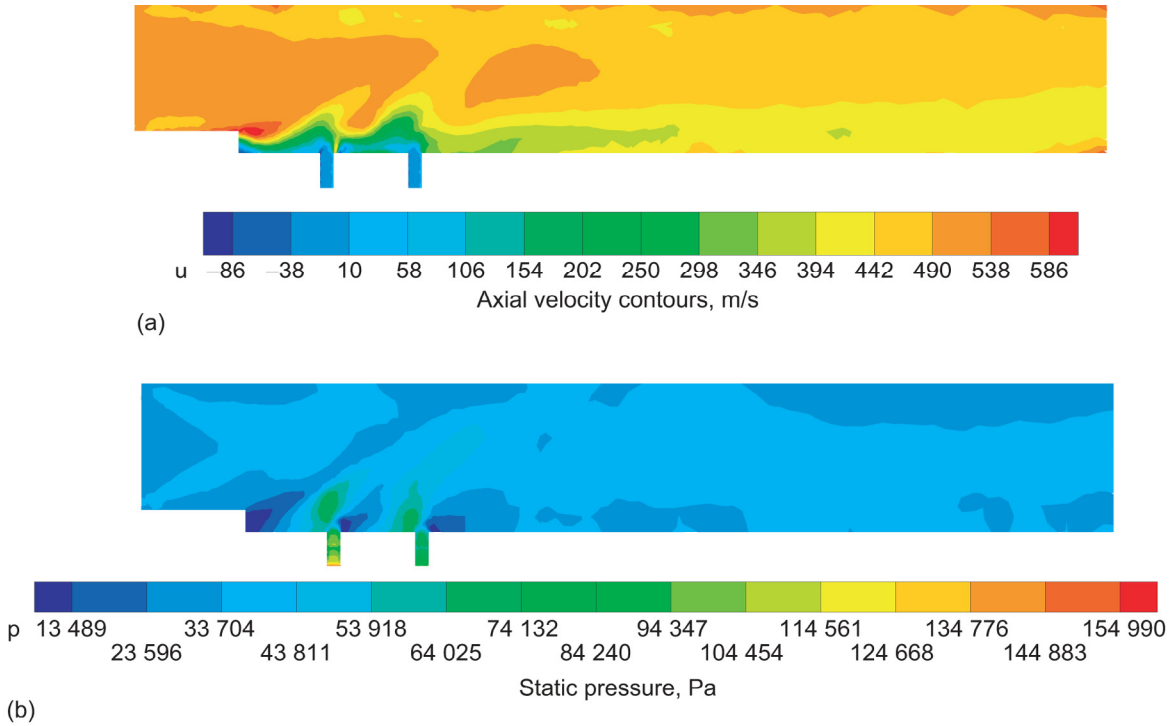

Figure 2.—NCC computed contours on plane containing the jet centerline, for staged transverse injection. (a) Axial velocity. (b) Static pressure.

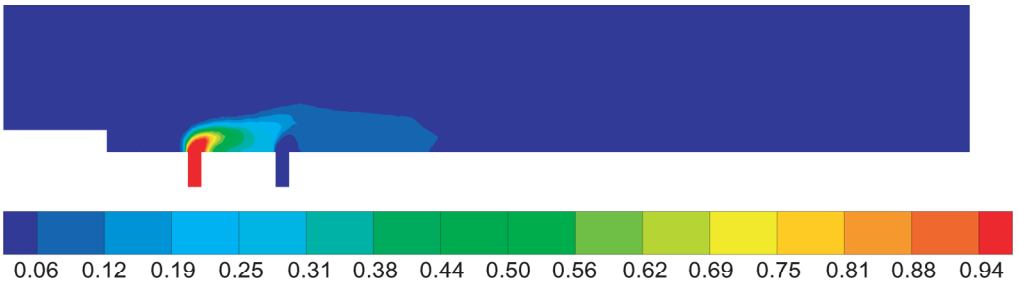

(a)

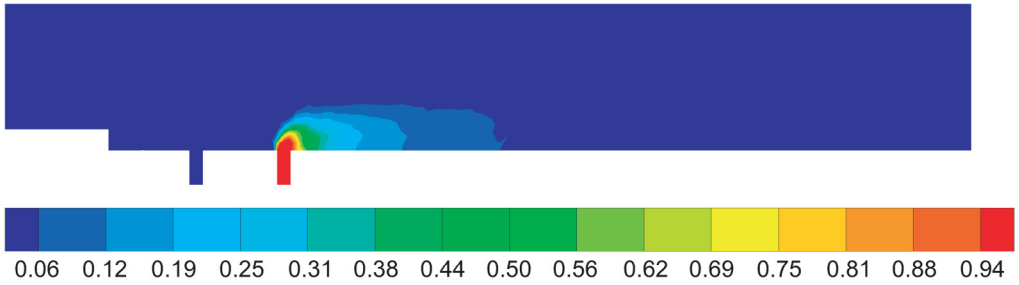

(b)

Figure 3.—NCC computed contours of marker concentrations indicating penetration distance into the main flow, for staged transverse injection. (a) Upstream jet. (b) Downstream jet.

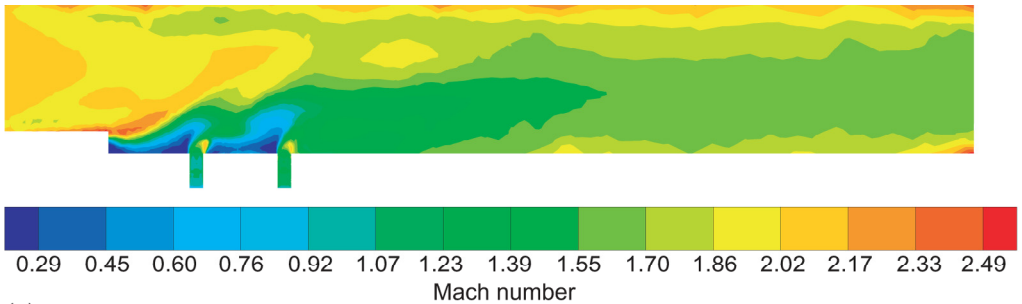

(a)

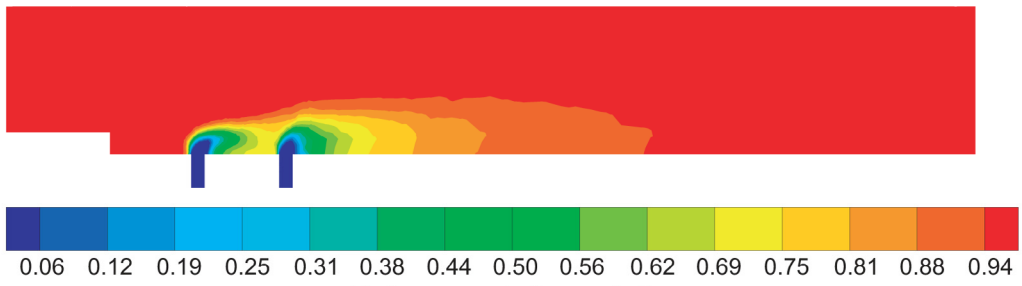

(b)

Figure 4.—NCC computed contours of the main flow, for staged transverse injection. (a) Mach number. (b) Marker concentration.

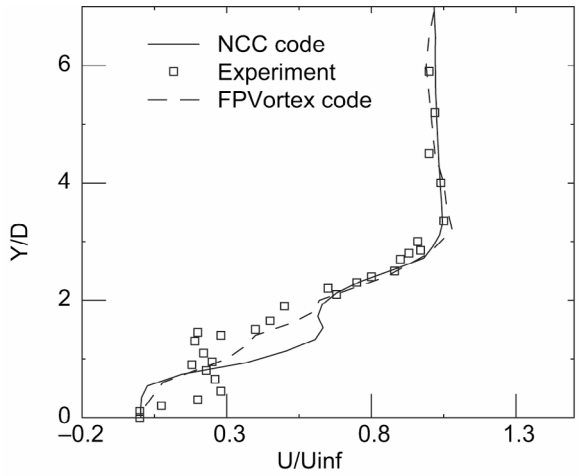

Figure 5.—Comparison of upstream injector normalized velocity data, for staged transverse injection. x/D = 0.0.

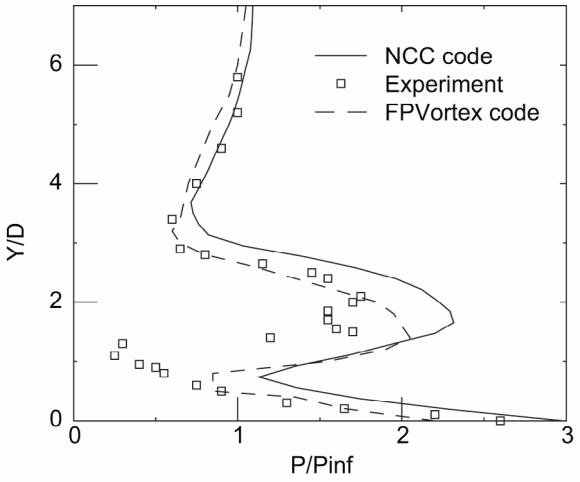

Figure 6.—Comparison of upstream injector normalized pressure data, for staged transverse injection. x/D = 0.0.

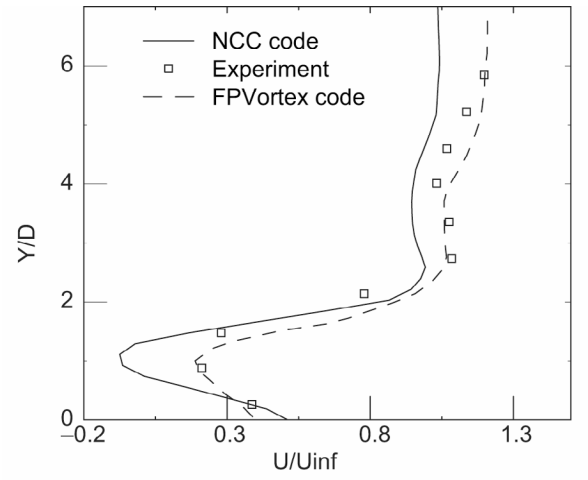

Figure 7.—Comparison of upstream injector normalized velocity data, for staged transverse injection. x/D = 3.0.

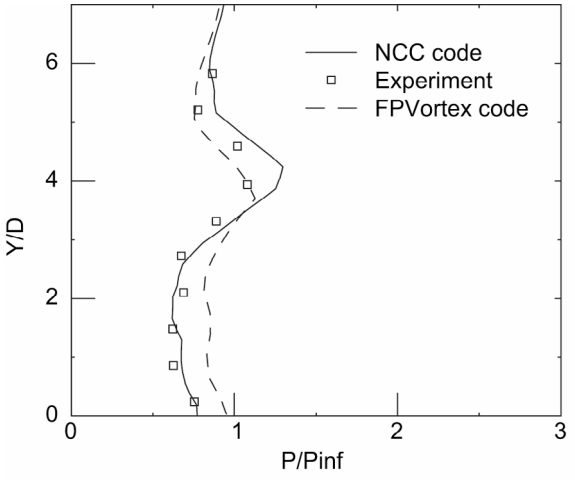

Figure 8.—Comparison of upstream injector normalized pressure data, for staged transverse injection. x/D = 3.0.

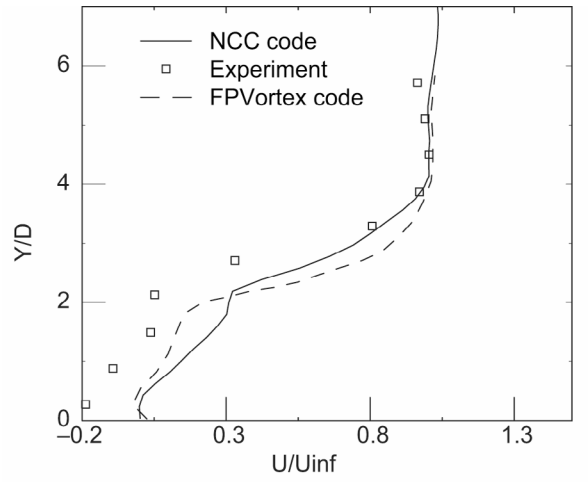

Figure 9.—Comparison of upstream injector normalized velocity data, for staged transverse injection. x/D = 6.0.

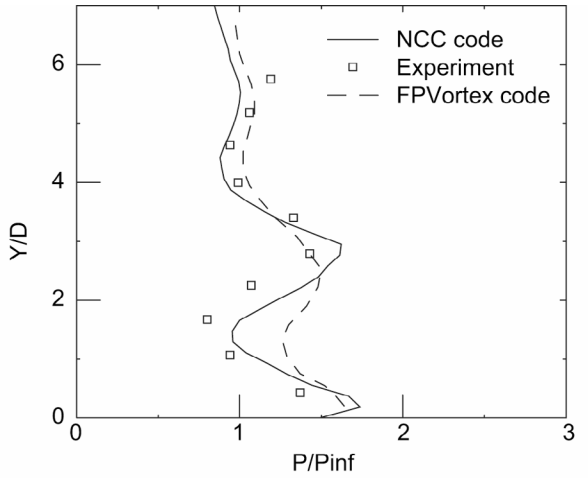

Figure 10.—Comparison of upstream injector normalized pressure data, for staged transverse injection. x/D = 6.0.

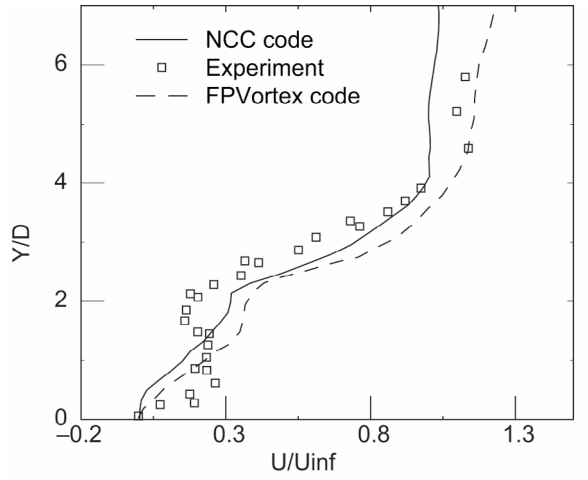

Figure 11.—Comparison of downstream injector normalized velocity data, for staged transverse injection. x/D = 6.6.

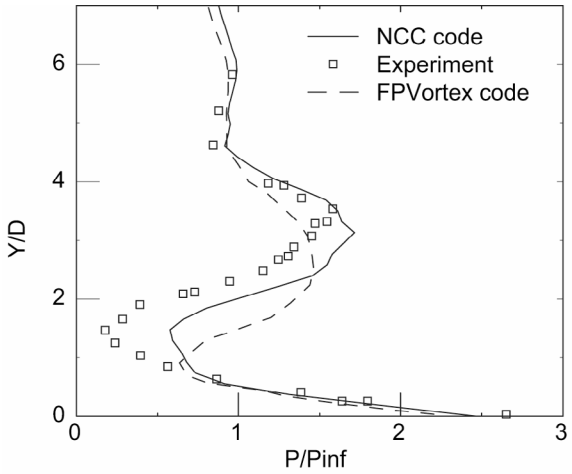

Figure 12.—Comparison of downstream injector normalized pressure data, for staged transverse injection. x/D = 6.6.

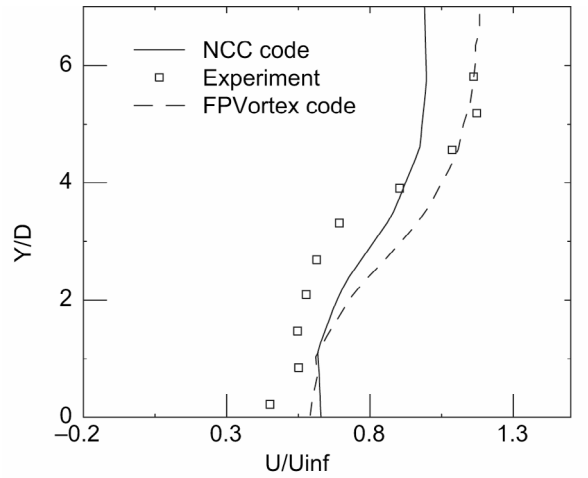

Figure 13.—Comparison of downstream injector normalized velocity data, for staged transverse injection. x/D = 12.8.

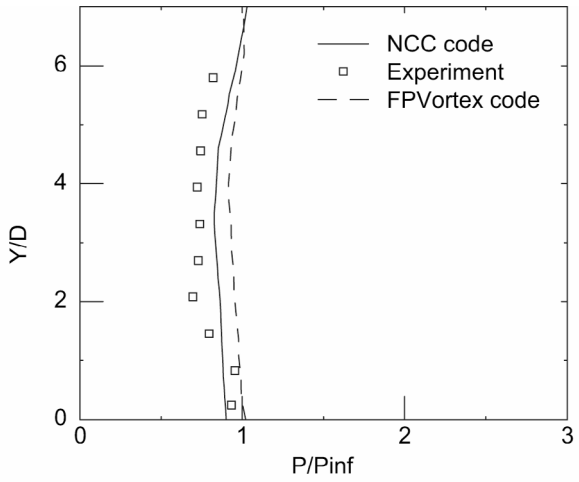

Figure 14.—Comparison of downstream injector normalized pressure data, for staged transverse injection. x/D = 12.8.

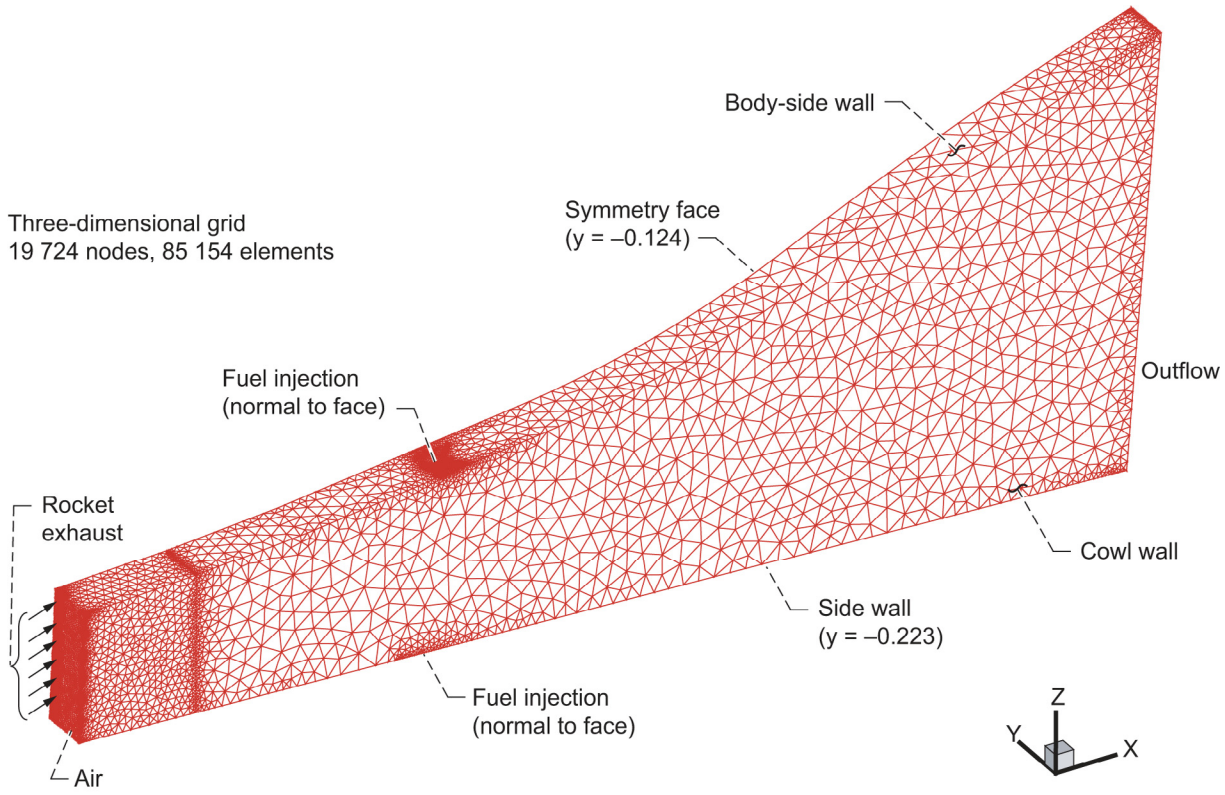

Figure 15.—Computational grid and schematic for RBCC combustor.

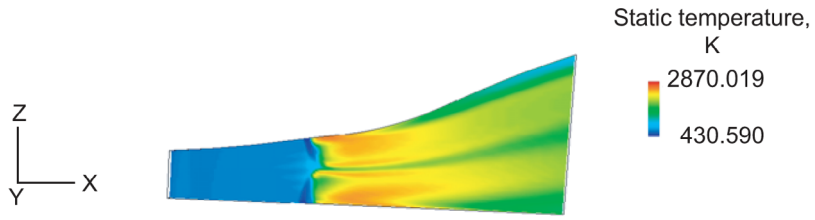

Figure 16.—VULCAN code temperature contour in a plane containing the injector centerline (Ref. [2]).

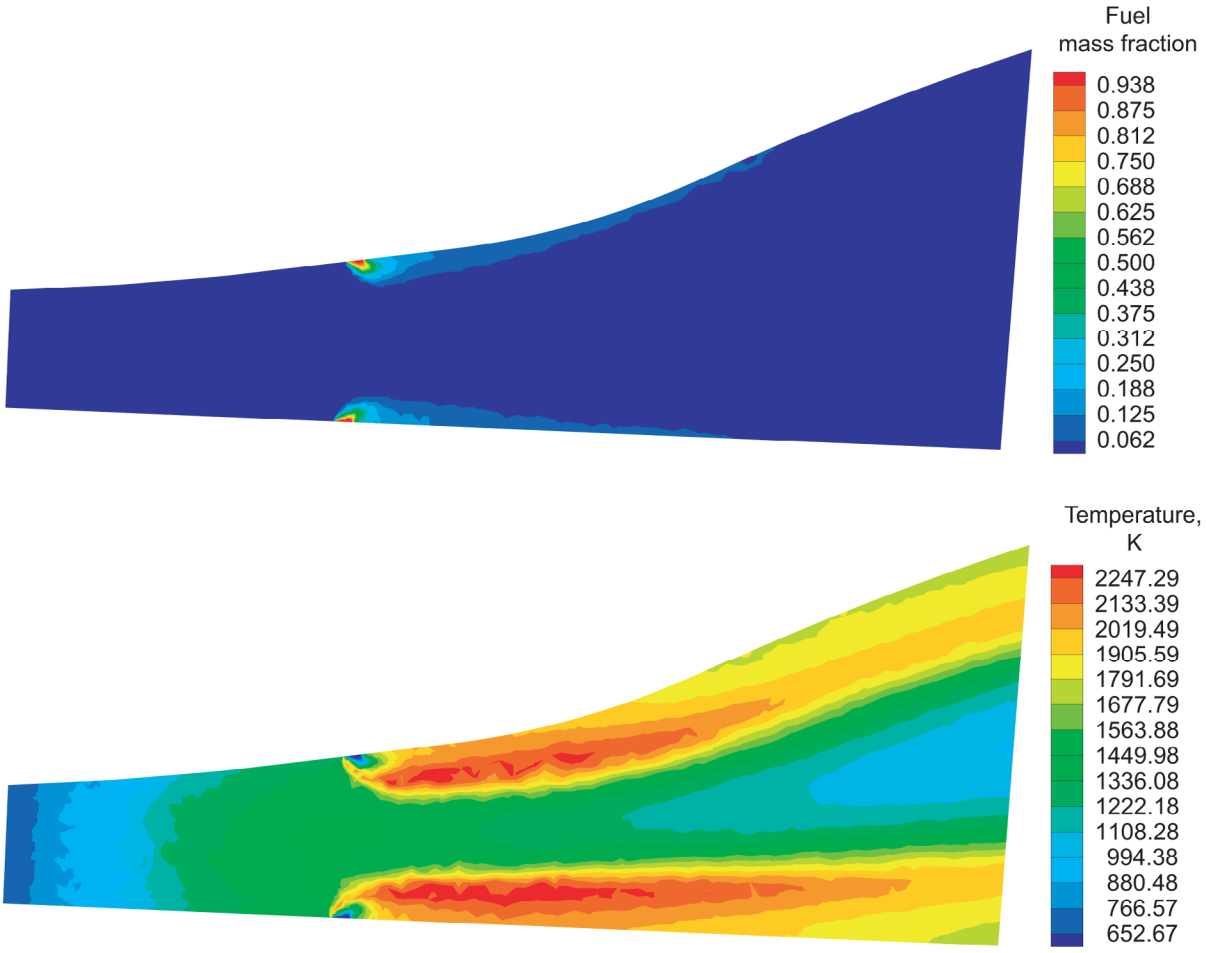

Figure 17.—NCC code coarse grid solution for RBCC combustor in a plane containing the injector centerline.

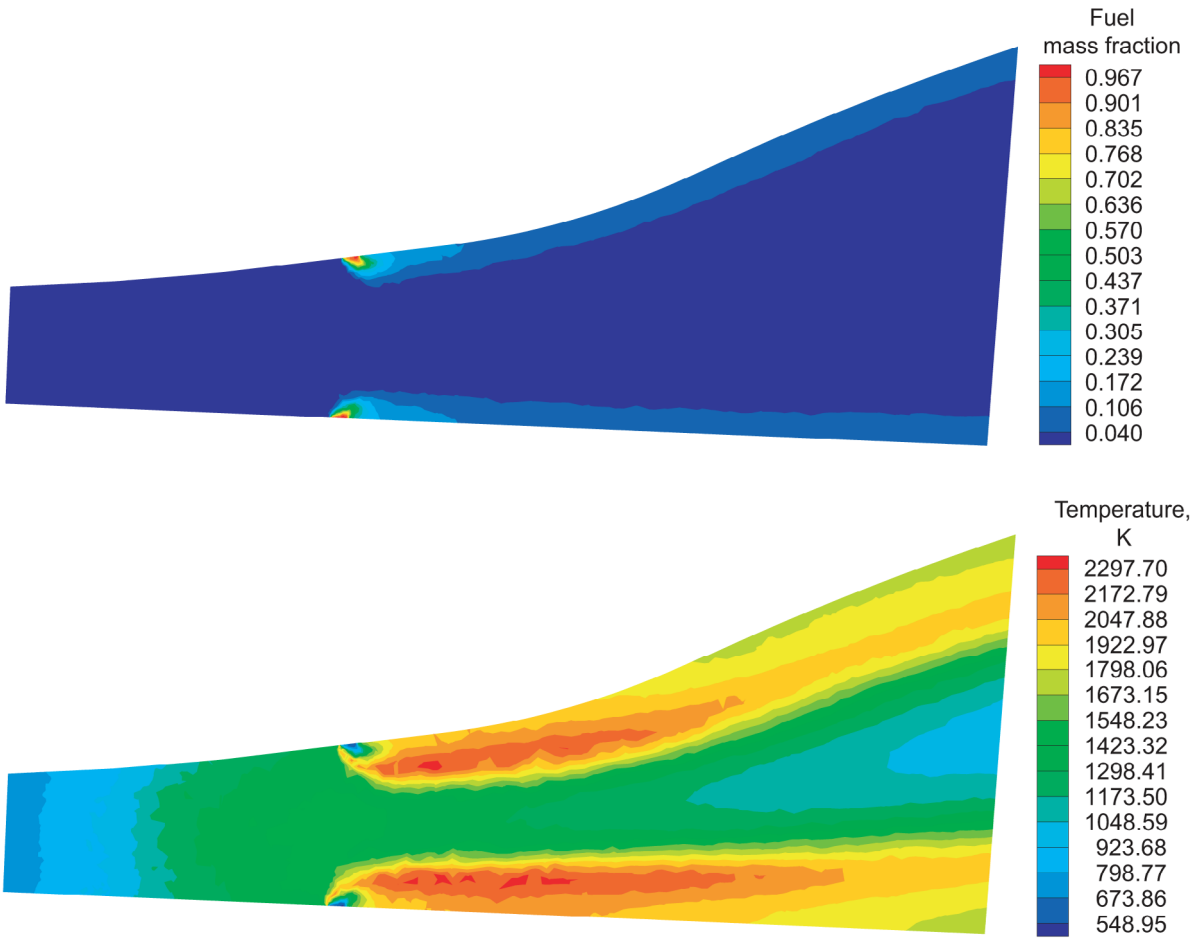

Figure 18.—NCC code fine grid solution for RBCC combustor in a plane containing the injector centerline.

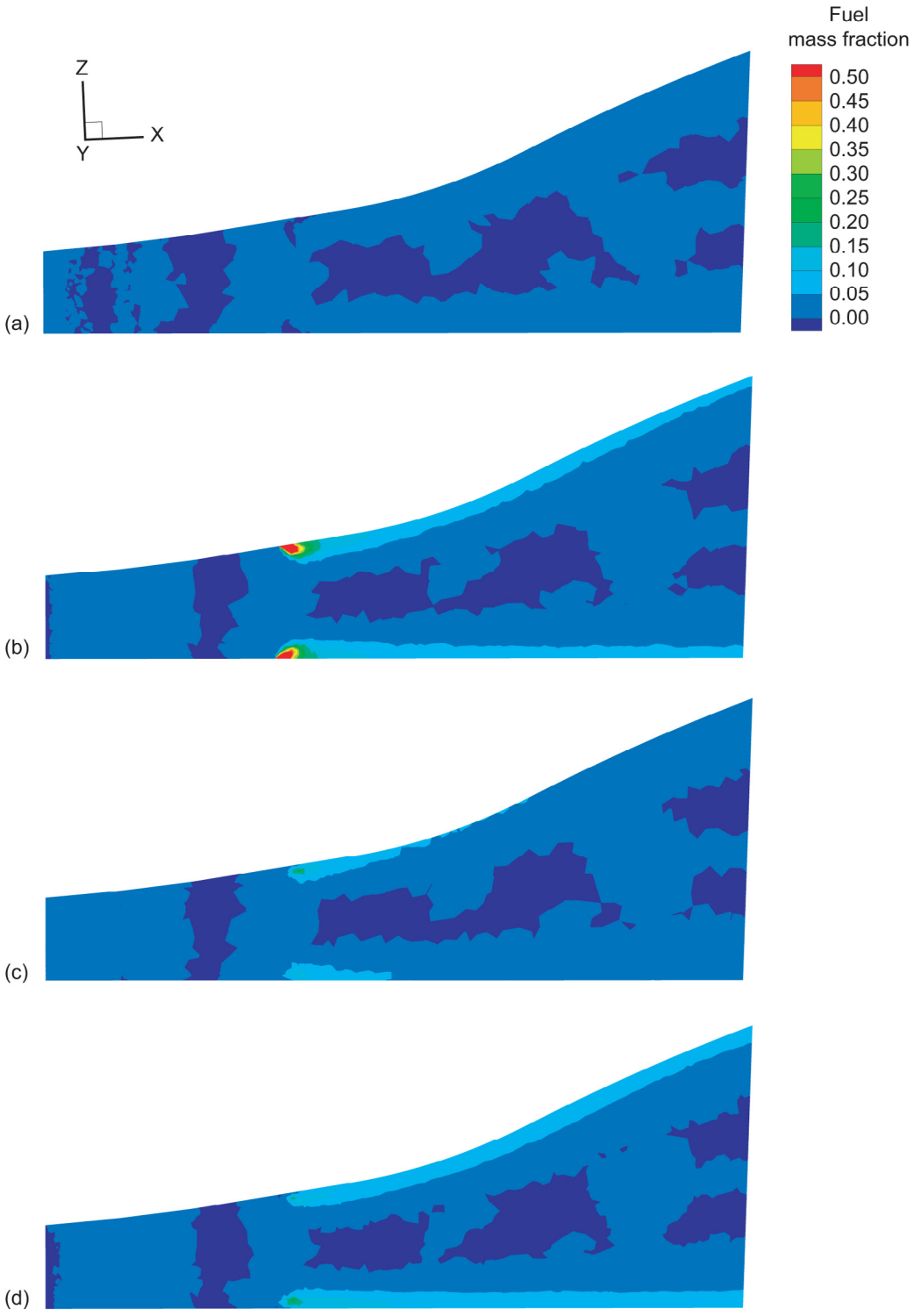

Figure 19.—NCC code fuel mass fraction for RBCC combustor at 4 spanwise locations. (a) Centerline of rocket plane (y/Y = 0.06). (b) Centerline of fuel injection plane (y/Y = 0.60). (c) Between rocket plane and fuel injection plane (y/Y = 0.36). (d) Between fuel injection plane and side wall (y/Y = 0.79).

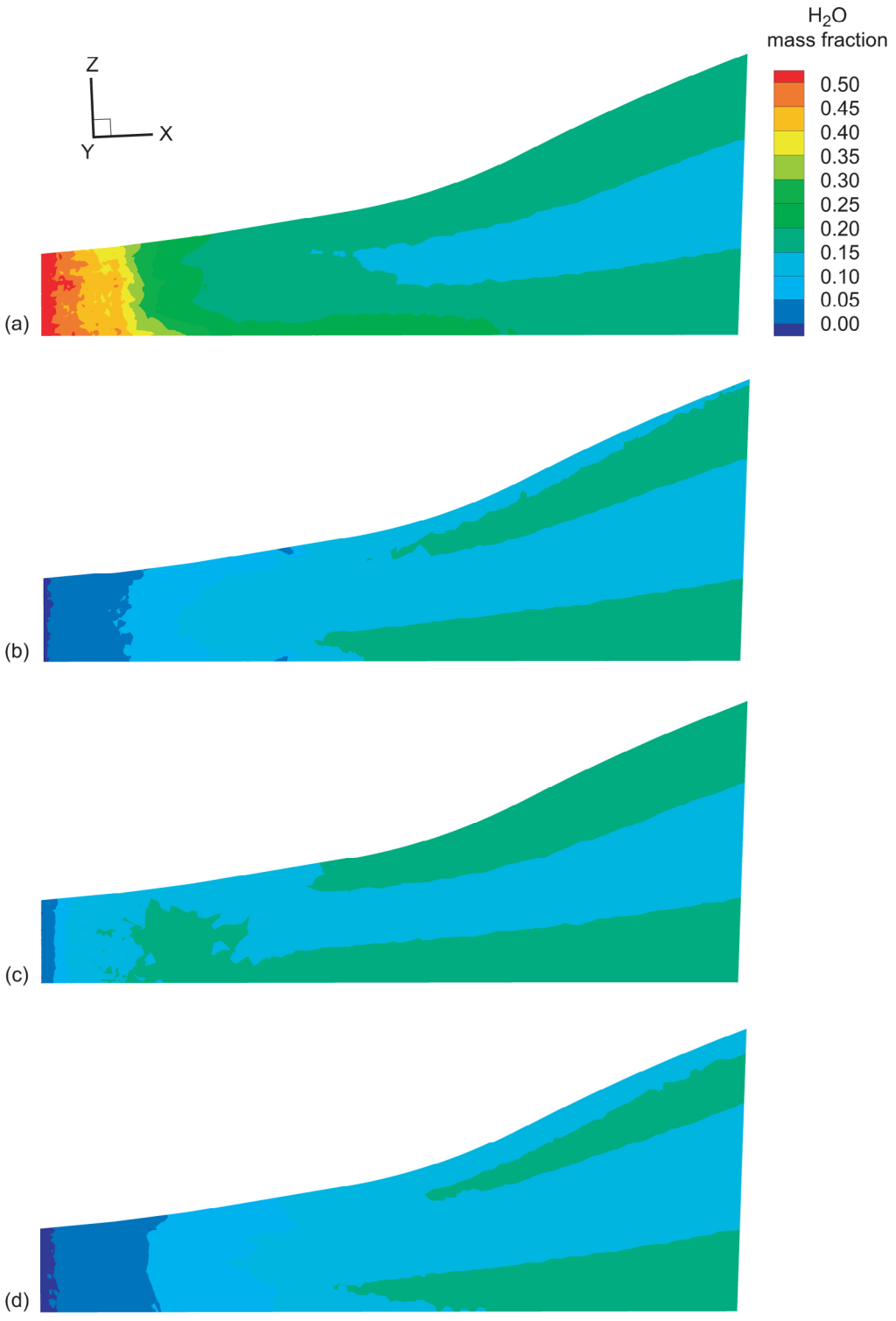

Figure 20.—NCC code H_2O mass fraction for RBCC combustor at 4 spanwise locations. (a) Centerline of rocket plane (y/Y = 0.06). (b) Centerline of fuel injection plane (y/Y = 0.60). (c) Between rocket plane and fuel injection plane (y/Y = 0.36). (d) Between fuel injection plane and side wall (y/Y = 0.79).

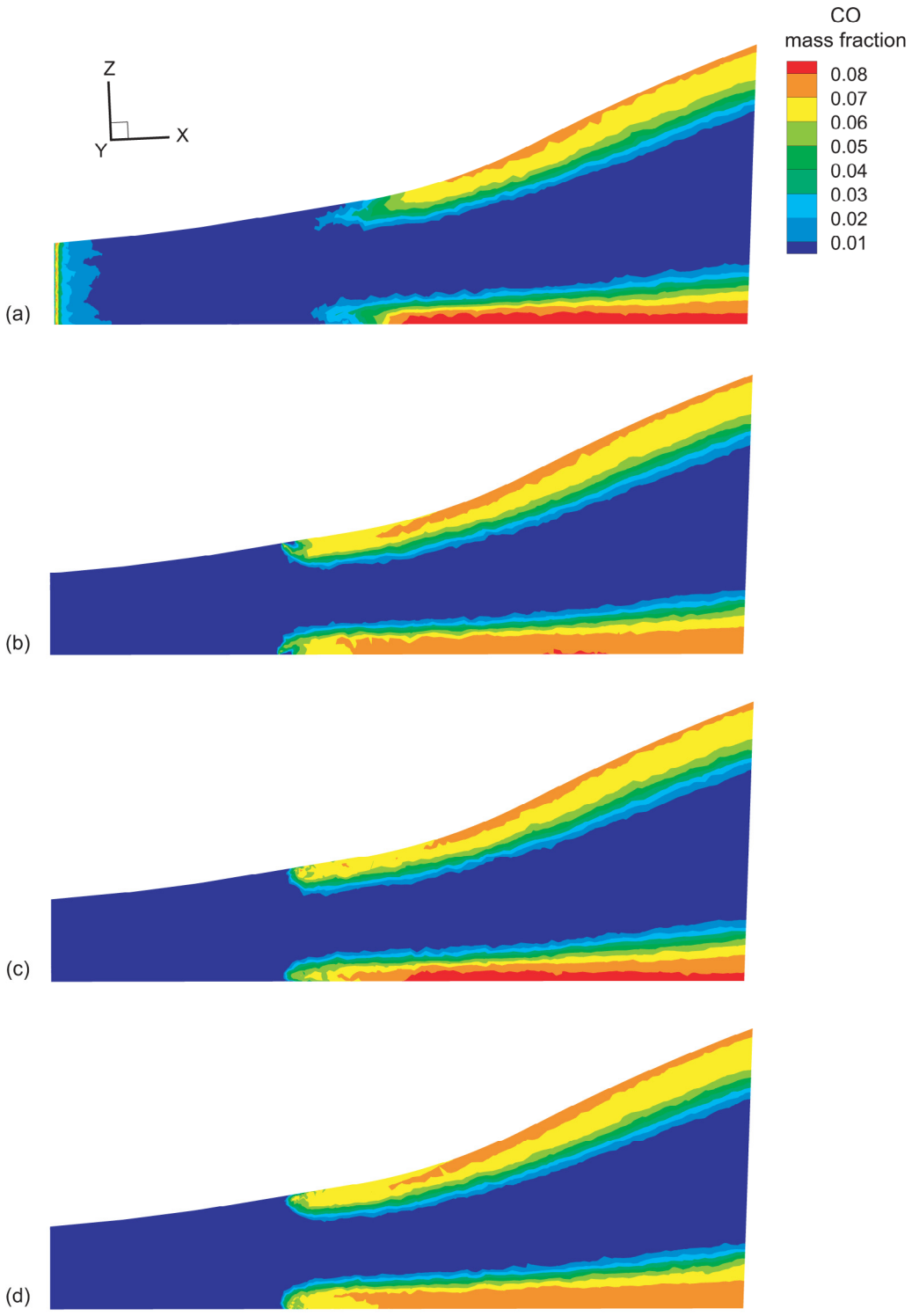

Figure 21.—NCC code CO mass fraction for RBCC combustor at 4 spanwise locations. (a) Centerline of rocket plane (y/Y = 0.06). (b) Centerline of fuel injection plane (y/Y = 0.60). (c) Between rocket plane and fuel injection plane (y/Y = 0.36). (d) Between fuel injection plane and side wall (y/Y = 0.79).

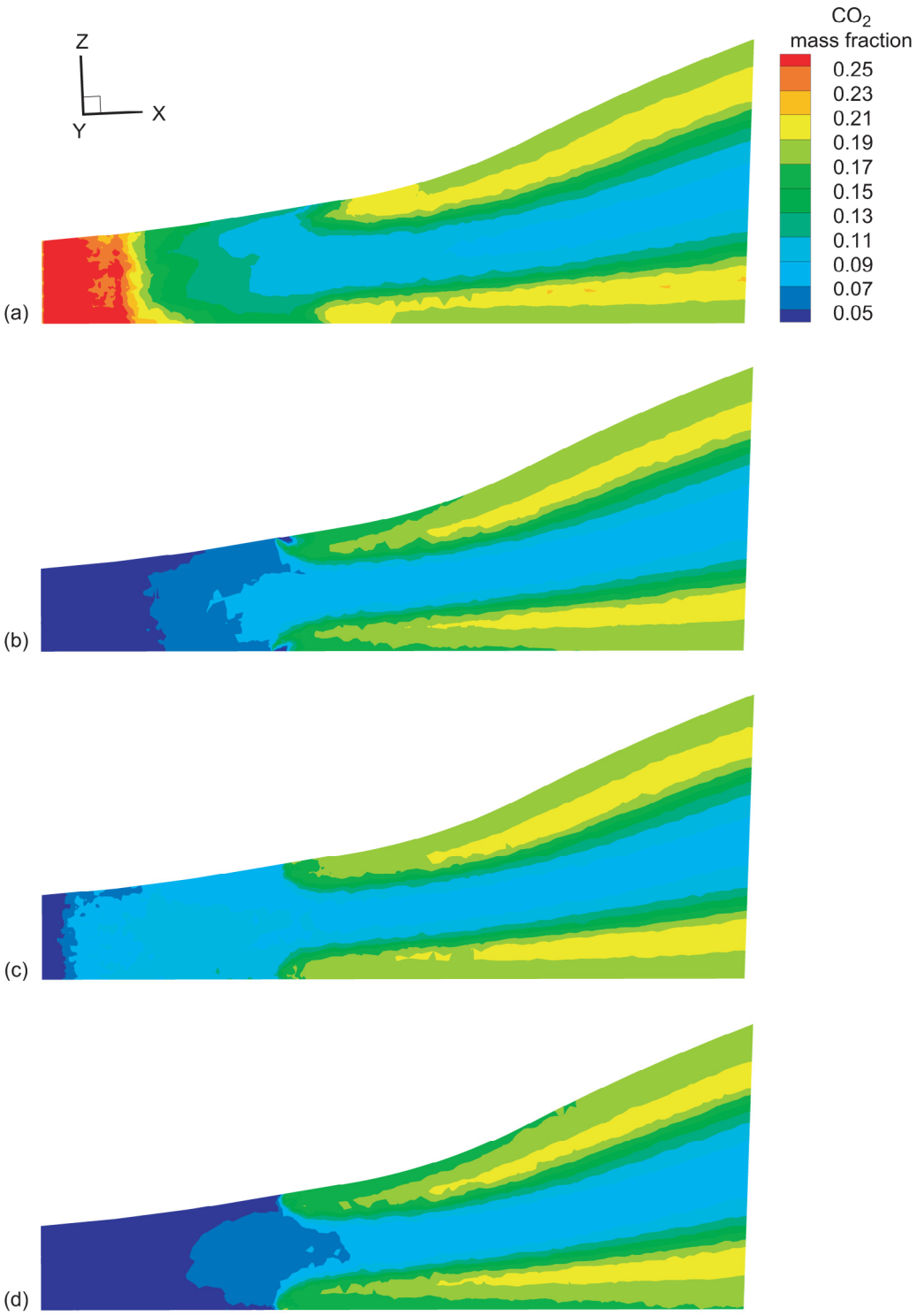

Figure 22.—NCC code CO_2 mass fraction for RBCC combustor at 4 spanwise locations. (a) Centerline of rocket plane (y/Y = 0.06). (b) Centerline of fuel injection plane (y/Y = 0.60). (c) Between rocket plane and fuel injection plane (y/Y = 0.36). (d) Between fuel injection plane and side wall (y/Y = 0.79).

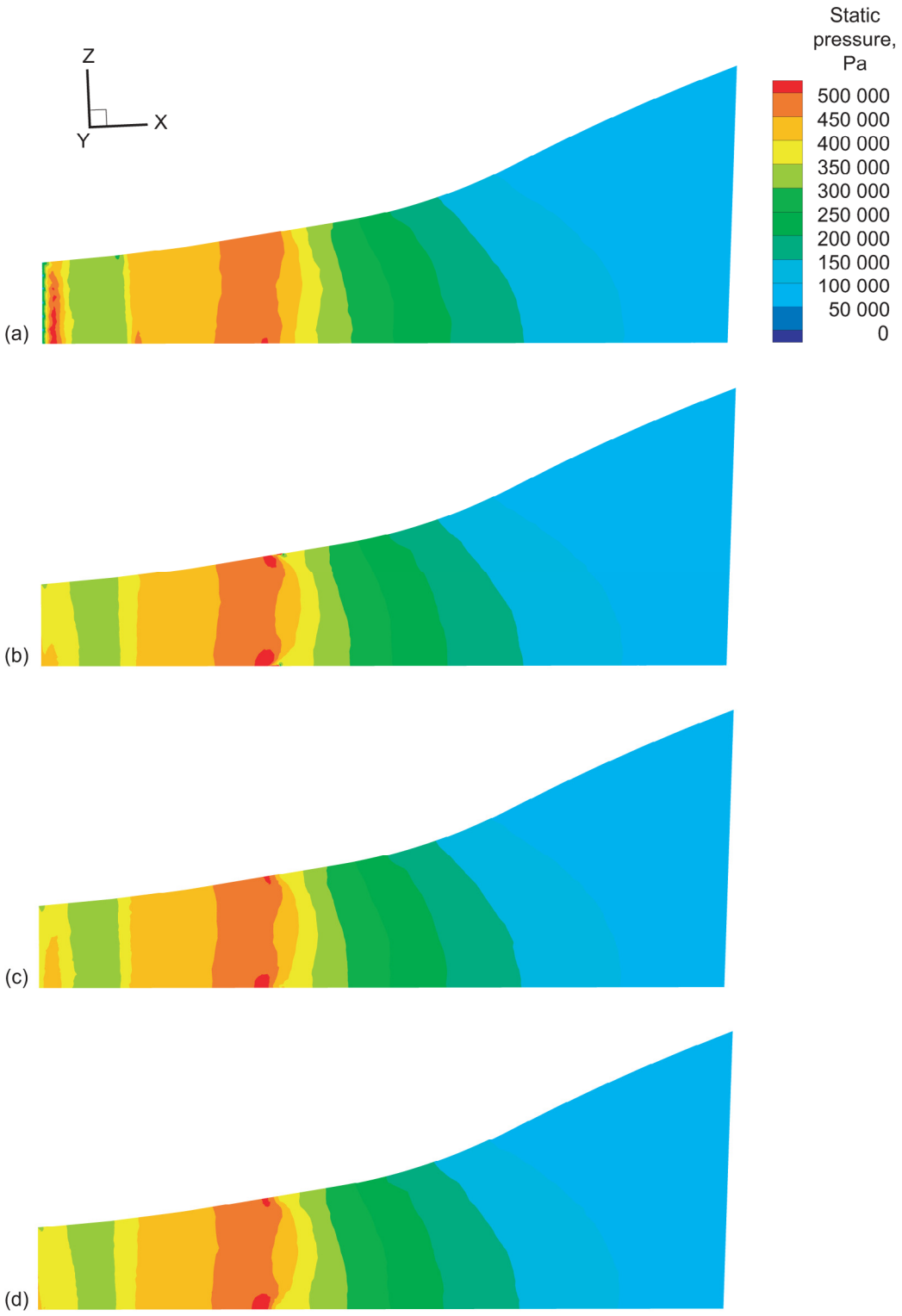

Figure 23.—NCC code pressure contours for RBCC combustor at 4 spanwise locations. (a) Centerline of rocket plane (y/Y = 0.06). (b) Centerline of fuel injection plane (y/Y = 0.60). (c) Between rocket plane and fuel injection plane (y/Y = 0.36). (d) Between fuel injection plane and side wall (y/Y = 0.79).

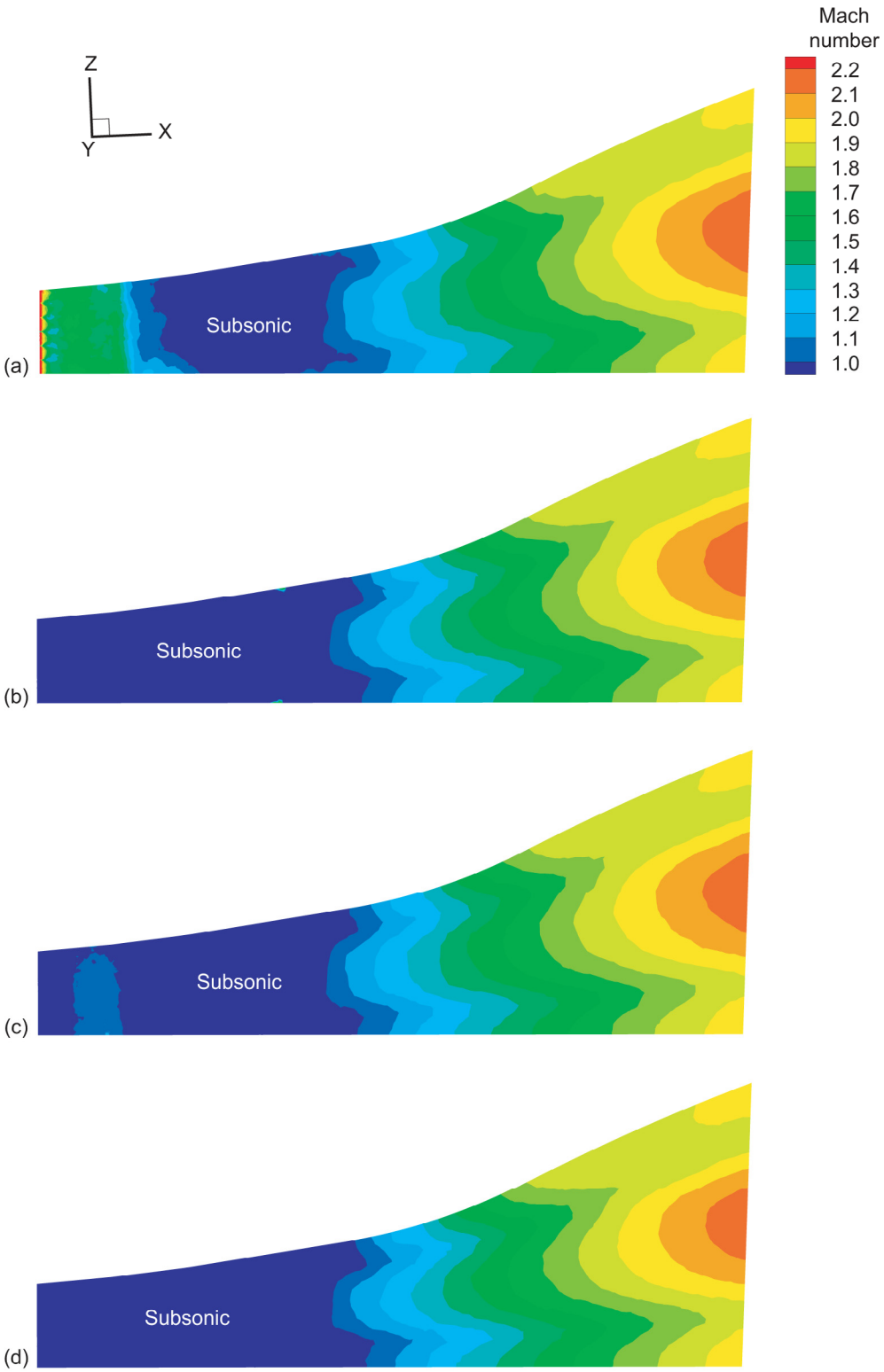

Figure 24.—NCC code Mach number contours for RBCC combustor at 4 spanwise locations. (a) Centerline of rocket plane (y/Y = 0.06). (b) Centerline of fuel injection plane (y/Y = 0.60). (c) Between rocket plane and fuel injection plane (y/Y = 0.36). (d) Between fuel injection plane and side wall (y/Y = 0.79).

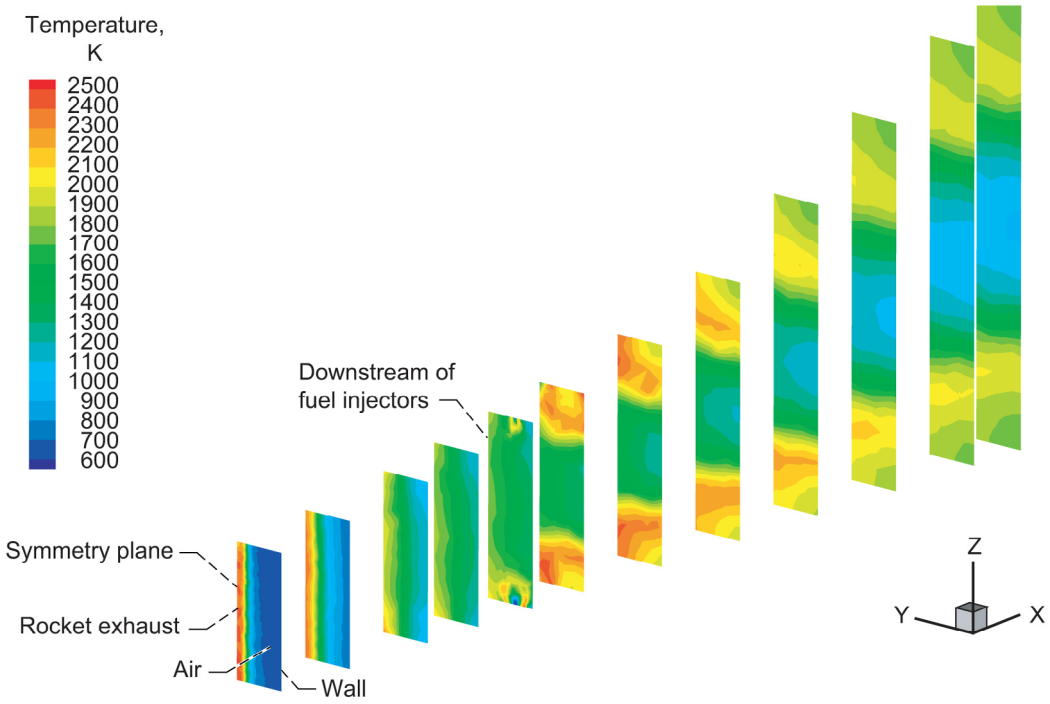

Figure 25.—NCC computed temperature contours for RBCC combustor at axial locations.

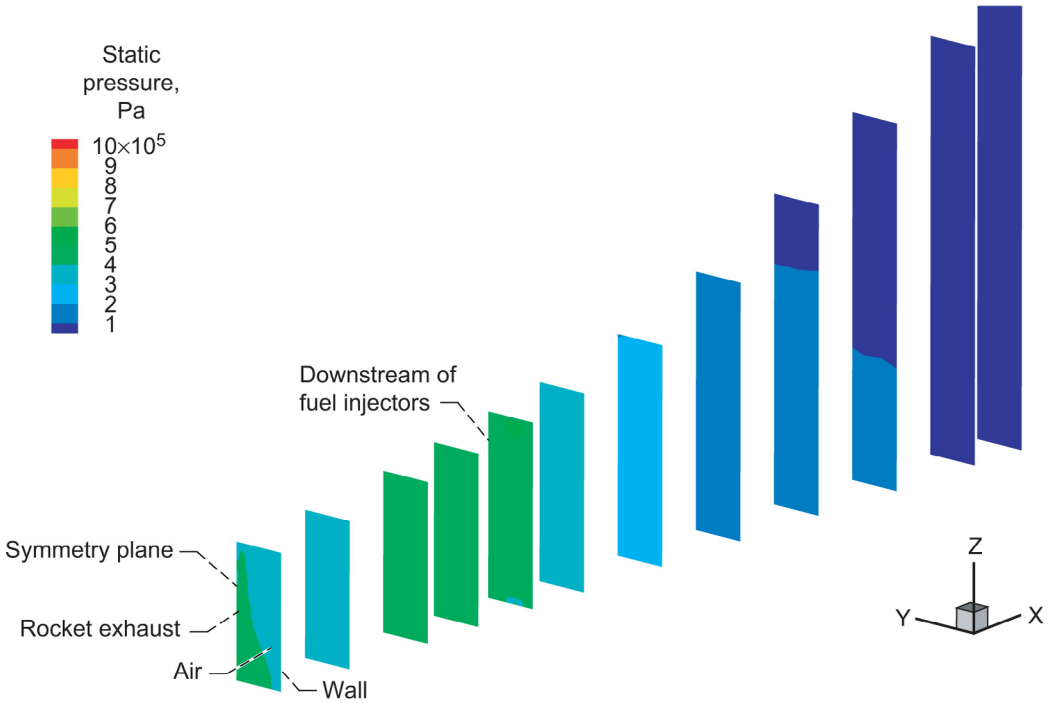

Figure 26.—NCC computed pressure contours for RBCC combustor at axial locations.

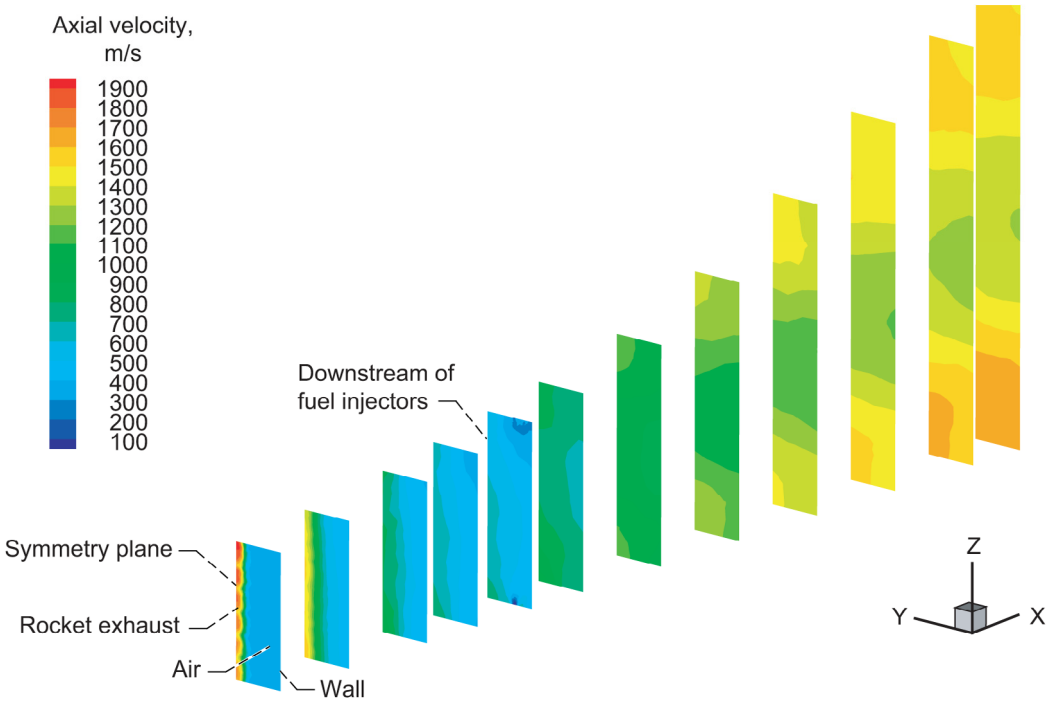

Figure 27.—NCC computed axial velocity contours for RBCC combustor at axial locations.

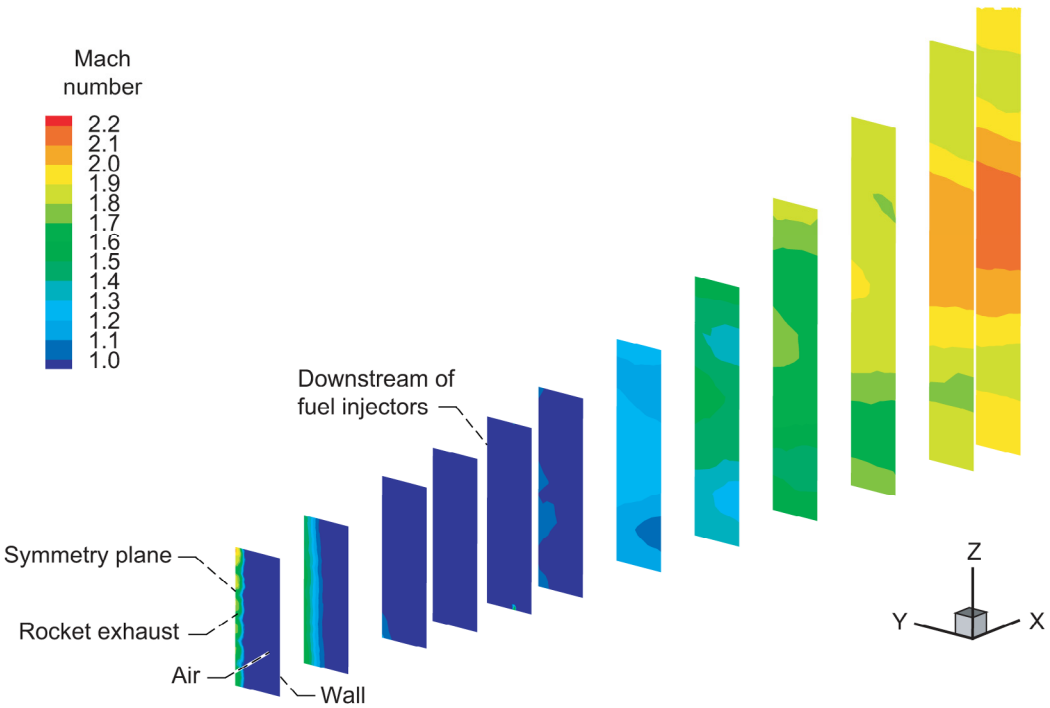

Figure 28.—NCC computed Mach number contours for RBCC combustor at axial locations.

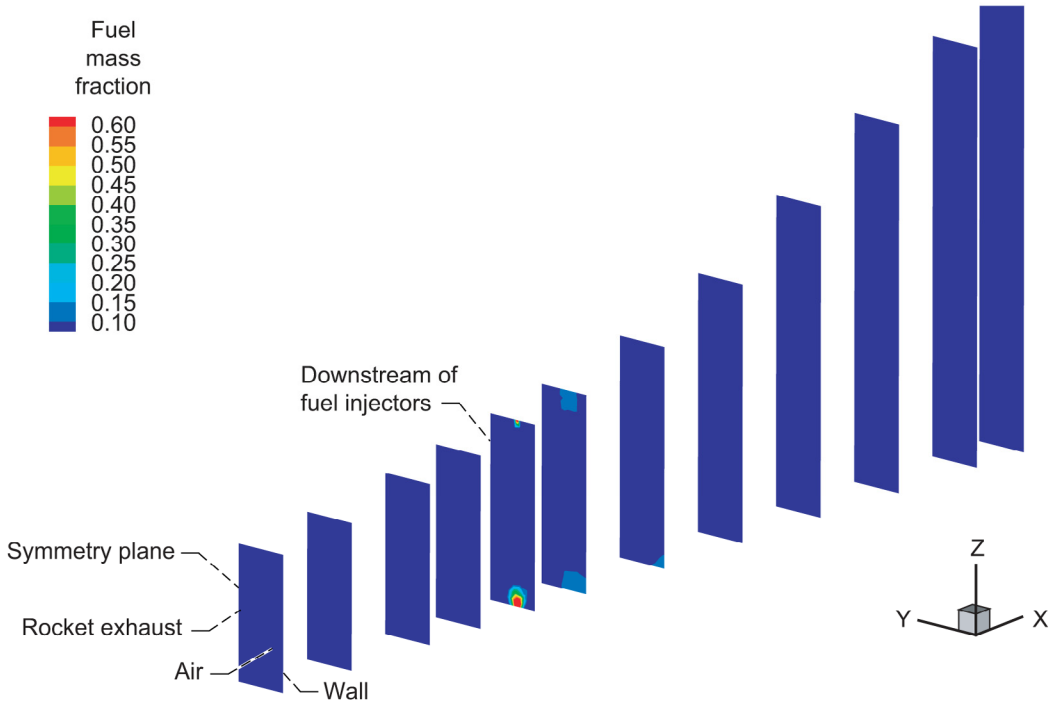

Figure 29.—NCC computed fuel mass fraction contours for RBCC combustor at axial locations.

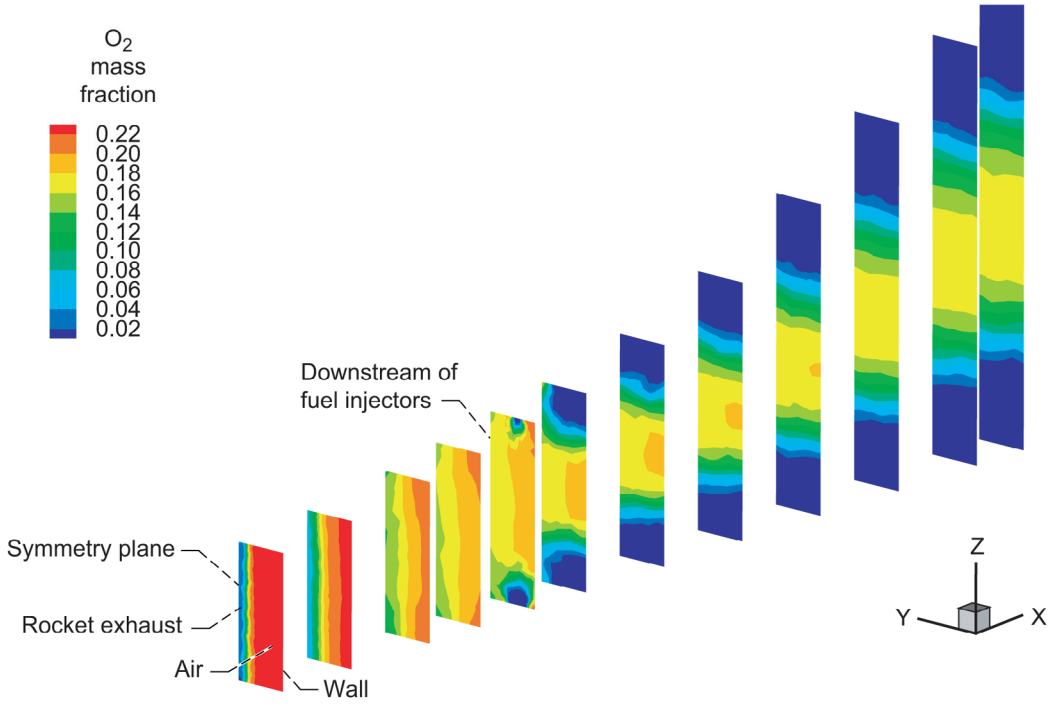

Figure 30.—NCC computed O_2 mass fraction contours for RBCC combustor at axial locations.

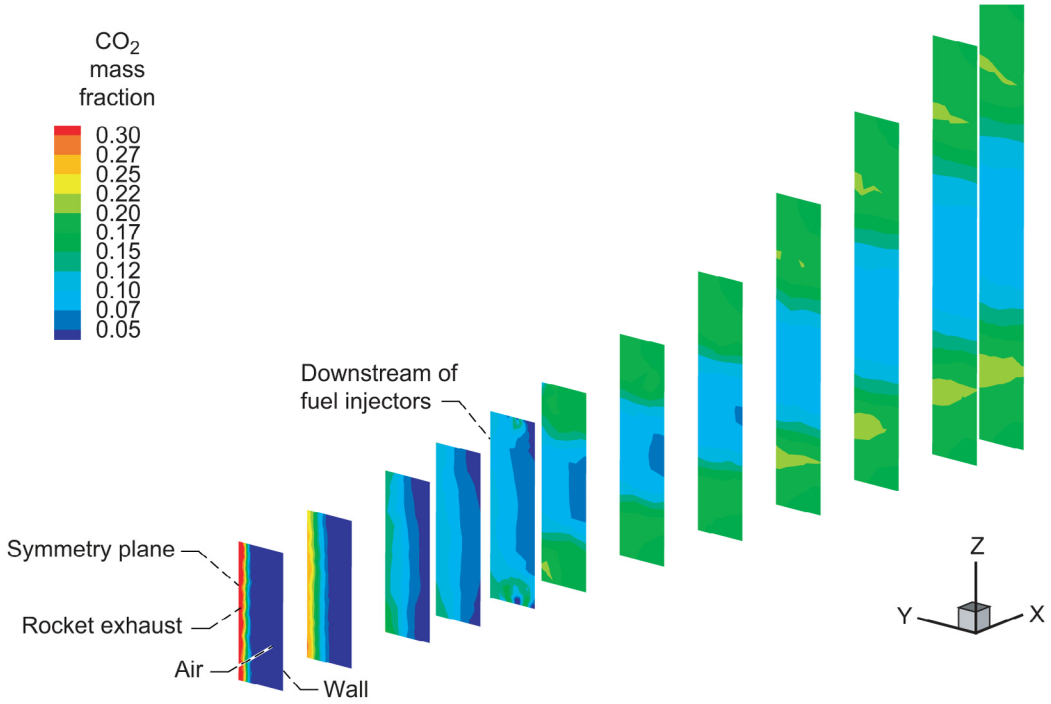

Figure 31.—NCC computed CO_2 mass fraction contours for RBCC combustor at axial locations.

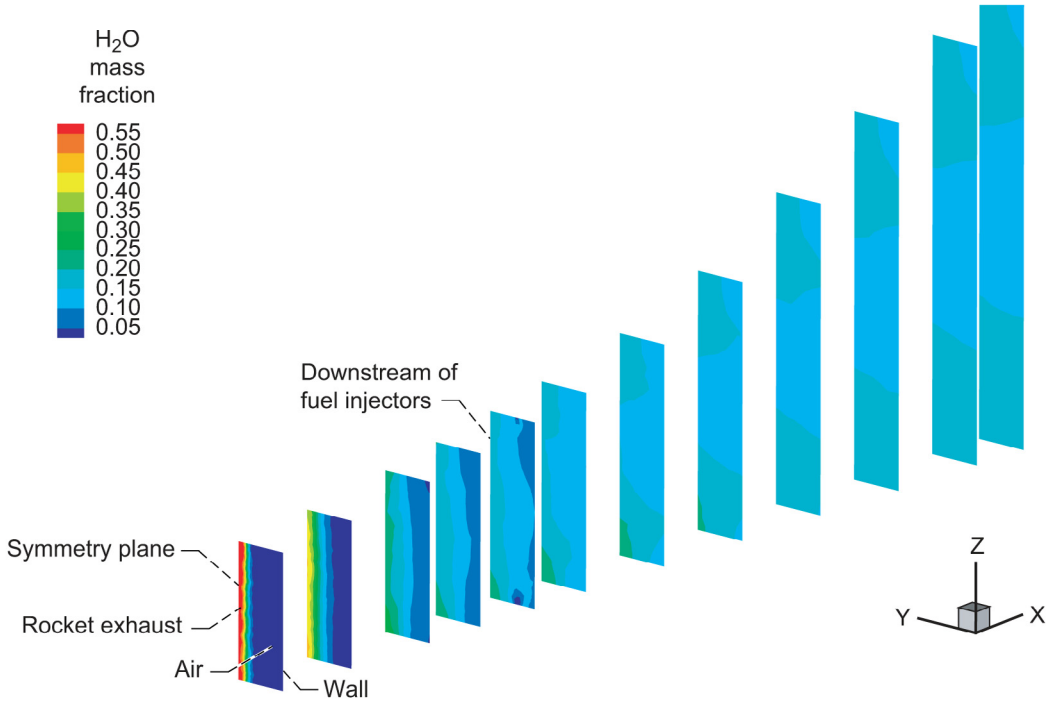

Figure 32.—NCC computed H_2O mass fraction contours for RBCC combustor at axial locations.

REPORT DOCUMENTATION PAGE

Form Approved
OMB No. 0704-0188

1. AGENCY USE ONLY (*Leave blank*)	2. REPORT DATE	3. REPORT TYPE AND DATES COVERED
	July 2005	Technical Memorandum

4. TITLE AND SUBTITLE

Validation of the NCC Code for Staged Transverse Injection and Computations for a RBCC Combustor

5. FUNDING NUMBERS

WBS–22–714–20–22

6. AUTHOR(S)

Kumud Ajmani and Nan-Suey Liu

7. PERFORMING ORGANIZATION NAME(S) AND ADDRESS(ES)

National Aeronautics and Space Administration
John H. Glenn Research Center at Lewis Field
Cleveland, Ohio 44135–3191

8. PERFORMING ORGANIZATION REPORT NUMBER

E–15135

9. SPONSORING/MONITORING AGENCY NAME(S) AND ADDRESS(ES)

National Aeronautics and Space Administration
Washington, DC 20546–0001

10. SPONSORING/MONITORING AGENCY REPORT NUMBER

NASA TM—2005-213647

11. SUPPLEMENTARY NOTES

Kumud Ajmani, Taitech, Inc., 1430 Oak Court, Suite 301, Beavercreek, Ohio 45430, email: kumud.ajmani@grc.nasa.gov; and Nan-Suey Liu, NASA Glenn Research Center, email: Nan-Suey.Liu@grc.nasa.gov. Responsible person, Kumud Ajmani, organization code RTB, 216–433–2671.

12a. DISTRIBUTION/AVAILABILITY STATEMENT

Unclassified - Unlimited
Subject Categories: 02 and 07

Available electronically at http://gltrs.grc.nasa.gov

This publication is available from the NASA Center for AeroSpace Information, 301–621–0390.

12b. DISTRIBUTION CODE

13. ABSTRACT ***(Maximum 200 words)***

The NCC code was validated for a case involving staged transverse injection into Mach 2 flow behind a rearward facing step. Comparisons with experimental data and with solutions from the FPVortex code were performed to assess the performance of the NCC code. The code was then used to perform computations to study fuel-air mixing for the combustor of a candidate rocket-based combined cycle engine geometry. Comparisons with a one-dimensional analysis and a three-dimensional code (VULCAN) were performed to assess the qualitative and quantitative performance of the NCC solver.

14. SUBJECT TERMS

Combustion chambers; Backward-facing steps; Injection; Spacecraft propulsion; Rocket-based combined-cycle engines

15. NUMBER OF PAGES

35

16. PRICE CODE

17. SECURITY CLASSIFICATION OF REPORT	18. SECURITY CLASSIFICATION OF THIS PAGE	19. SECURITY CLASSIFICATION OF ABSTRACT	20. LIMITATION OF ABSTRACT
Unclassified	Unclassified	Unclassified	